DESIGN AND ANALYSIS OF FULL-SCALE OFFSET STIFFENED-SPRING BACK REFLECTOR

Ömer Soykasap*
Department of Mechanics,
Afyon Kocatepe University, Gazligol Yolu, Ayfonkarahisar, 03200, Turkey,
soykasap@aku.edu.tr

Lin Tze Tan†
Department of Civil & Environmental Engineering,
University College London, Gower Street, London WC1E 6BT, UK,
l.tan@ucl.ac.uk

ABSTRACT

This paper presents the design and analysis of a novel 6 m diameter offset Stiffened Spring-Back Reflector together with the testing of a 0.8 m technology demonstrator. Not only do we demonstrate the feasibility and effectiveness of the Stiffened Spring-Back Reflector concept, but we also show that a large scale offset version of the Stiffened Spring-Back Reflector (SSBR) is able to meet –and sometimes better– the stringent specifications of large high accuracy communications reflector antennas. The SSBR is a monolithic thin carbon-fibre-reinforced-plastic shell which is stiffened along the edge by an integral elastically collapsible stiffener. This collapsible stiffening rim significantly increases the overall stiffness of the dish in the deployed state and yet its configuration is such that the structure can still be packaged elastically.

The 0.8 m diameter technology demonstrator has a large initial resistance against packaging of about 117 N/m with good surface accuracy for a mass of less than 100 grams. While the full-scale 6 m diameter offset reflector has an rms surface accuracy under thermal loading, modal behaviour, linear dynamic transient response, static buckling condition and stress distribution which are well within the limits specified for Ku band reflectors. The Stiffened Spring-Back Reflector has a mass of 25.5 kg, maximum rms due to thermal distortions of 3.5 μm and a natural frequency of 1.66 Hz.

1. INTRODUCTION

Future telecommunication space missions require larger (4-8 m) and higher precision space borne reflector antennas, while earth observation and scientific missions require even higher frequency operation. The recent European Space Agency sponsored Technical Assessment of High Accuracy Large Space Borne Reflector Antenna (TAHARA) was conducted to assess the current state of the art concepts for large (6 m diameter) high precision antennas. Tan's Stiffened Spring Back Reflector (SSBR)[3], which had the lowest mass and highest deployed stiffness, emerged as one of the winning designs [1].

The SSBR is a flexible-shell structure that is folded elastically, see Fig.1. These reflectors are constructed as a single piece, without any joints or hinges, and hence are relatively inexpensive to manufacture. The folding concept is both simple and effective –opposite edges of the reflector are pulled towards each other by about half their original distance and are held by tie cables. The antenna is designed to fit in the normally unused space at the top of the rocket fairing or around the payload, its largest stowed dimension being slightly larger than the deployed diameter. Once in orbit, the tie cables that hold the reflector in its packaged configuration are released by pyrotechnic charges and the reflector deploys dynamically by releasing its stored elastic strain energy.

Key to the design of the SSBR is an integral collapsible stiffener [4] which significantly increases the overall stiffness of the dish in the deployed configuration and yet when it is being packaged, localized buckles form in the rim and hence reduce the overall stiffness of the structure allowing it to be folded elastically, without any hinges or motors. The behaviour of these localized buckles in the stiffener is dictated by two pairs of circumferential slits located perpendicularly to each other, Fig. 2.

Previous work by Tan et.al. [5] has shown that hinge slit angles are crucial in allowing large portions of the dish to bend when the reflector is being packaged – therefore reducing peak strains in the dish. Hence in general, these hinge slits dictate the peak stress in the dish and the final packaged force of the reflector. On the other hand, load slits allow the stiff-

*Associate Professor
†Lecturer in Structural Mechanics

FIG. 1: Stiffened Spring Back Reflector Demonstrator.

ener/skirt to buckle elastically during packaging and hence in general control the peak snapping load. Altering the length of these slits hence gives one the ability to tune the stiffness of the reflector as desired. Other adjustable parameters of the SSBR's stiffener are the stiffener width, angle of connection and thickness, see Fig. 2.

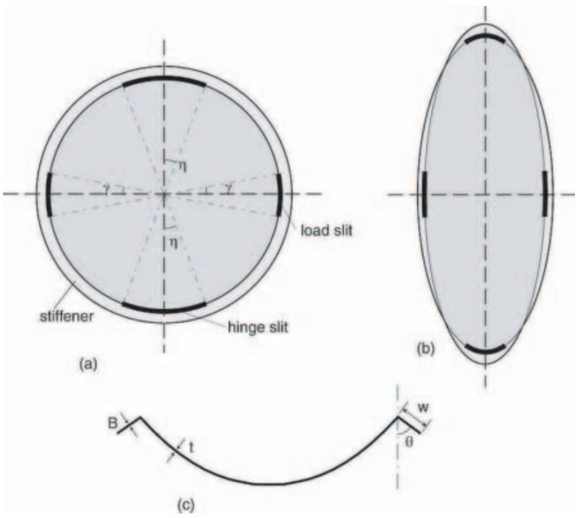

FIG. 2: Adjustable Parameters of the Stiffening System.

2. FULL-SCALE SSBR ANALYSES

In this study, Tan's optimised design for a 4.6 m diameter reflector [5] is scaled up to a 6 m diameter reflector with a focal length of 4.8 m and an offset of 0.3 m. The reflector structure is assumed to be made of triaxially woven CFRP with T300 fibres, composite modulus 30 GPa, Poisson's ratio 0.5, density 920 kg/m^3. Fig. 3 show the details of the model. The model consists of a reflector shell with a thickness of 0.39 mm; a flat skirt with a width of 130 mm and a thickness of 1.95 mm, and with a load slit angle of 14 deg, and a hinge slit of 28 deg; a rim reinforcement, 36 radial ribs, 18 clockwise and 18 anticlockwise spiral reinforcements. All reinforcements are assumed to be symmetric when projected onto the xy plane and are 40 mm wide and 0.66 mm thick, and a central reinforcement with a diameter of 0.913 m, and a thickness of 1.98 mm.

The reflector is modeled as a 3D shell structure in the ABAQUS Finite Element Analysis Software [6]. Each part is created separately, and then assembled together in the assembly module. All reinforcing elements are rigidly tied to the reflector shell. The assembly is then meshed with 3-node triangular general-purpose shell elements (S3). The model has 6688 elements for the reflector shell.

The need for reinforcements is investigated by considering two equal mass options: (i) a reflector with the reinforcement pattern shown in Fig. 3, and (ii) a reflector without reinforcements but with a smoothed over homogenously thicker dish and skirt. Both reflectors are assumed to be connected to a rigid interface at the center. The advantage of the reinforcements is demonstrated by the fact that the natural frequency of the reinforced reflector is 3.4 times higher than that of the equal mass homogenous thickness reflector.

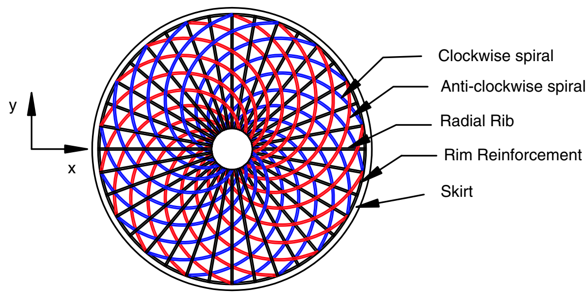

FIG. 3: Configuration of the Full-Scale SSBR.

Five different types of analyses are carried out to ascertain the performance of the reflector.

2.1. Thermal Analyses

Thermal distortion analyses were performed to determine the rms errors, resulting from several different in orbit thermal load cases. The single and combined load cases applied are:

- LC1 is a gradient along x-direction of 100°C over the total length of the reflector

- LC2 is gradient through the thickness of 0.1°C/mm (along the direction normal to the surface of the reflector)
- LC3 is a uniform absolute temperature of -150°C
- LC4 is a uniform absolute temperature of 170°C
- LC1 + LC2 + LC3 i.e. x-direction and through-thickness gradients combined with an absolute *low* temperature
- LC1 + LC2 + LC4 i.e. x-direction and through-thickness gradients combined with an absolute *high* temperature

For these thermal distortion analysis the SSBR is assumed to have free boundary conditions. The coefficient of thermal expansion (CTE) of the triaxially woven material was taken from experimentally measured values $\alpha_x = \alpha_y = -0.2 \times 10^{-6}/°\mathrm{C}$. The corresponding rms error of the distorted reflector is obtained with respect to the best-fit paraboloid. This best-fit paraboloid is calculated on the basis of the following four parameters:

- F: focal length of the best fit surface
- α : 1st rotation about the x-axis transforming (x,y,z) into (x',y',z')
- β : 2nd rotation about the y'-axis transforming (x',y',z') into (x",y",z")
- k_0 : translation of the vertex along z" direction

2.2. Modal Analyses

The eigenmodes and corresponding frequencies of the SSBR reflector mounted in two different conditions (i) the reflector fixed at its geometric centre as well as (ii) the reflector centrally attached to a boom which is then connected to the spacecraft.

In case (i), it is assumed that all the nodes of the dish within a diameter of 200 mm from the geometric center are fixed. While for case (ii) the basic geometry of the boom is illustrated in Fig. 4. The boom consists of three circular tubes and three hinges. The hinges are represented by lumped masses of 4 kg each, with the following associated stiffnesses: $K_x = K_z = 1{\times}10^8$ N/m, $K_y = 1{\times}10^7$ N/m, $K_{rx} = K_{rz} = 1{\times}10^6$ Nm, $K_{ry} = 1{\times}10^5$ Nm. The tubes have a diameter of 200 mm, a wall thickness of 2 mm, and differing lengths of L0 = 1.4 m, L1 = 3.626 m, L2 = 0.652 m. The boom which is modelled as a beam in Abaqus is constructed from an isotropic material with an elastic modulus of 90 GPa, and a Poisson's ratio of 0.33. It is connected to the center of the reflector at one end and the spacecraft at the other. For a more realistic representation of the connection between the boom and the reflector, multipoint constraints were applied to all reflector nodes within a 200 mm diameter of the reflector's geometric center. These nodes are then connected to a reference point at the center, which is in turn connected to the end of the boom via hinge H3 (Fig. 4).

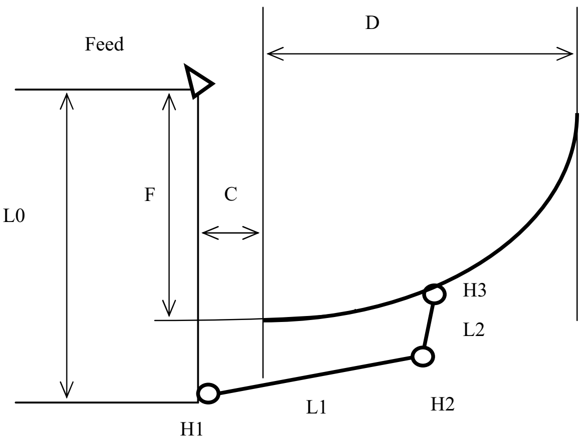

FIG. 4: Basic Definitions of the Boom Attachment.

2.3. Dynamic Transient Analyses

The sensitivity of the SSBR due to in-orbit disturbances, e.g. thruster impulses can be determined by the maximum defocusing of the reflector in response to sudden accelerations. Hence linear transient dynamic analyses are performed to estimate the time response of the SSBR and focal point displacements. The analyses are performed by applying unit step (translational) acceleration inputs independently in each of the global directions x, y, z. The corresponding response of the SSBR is determined by means of a modal analysis, superposing the time responses of the first 20 modes and using 1% modal damping in each mode.

2.4. Static Buckling Analyses

As an added measure, static buckling analyses were performed to determine which components of the reflector are most prone to buckling. Unit translational acceleration loads are applied statically and independently in the x, y, z directions in order to define the critical load factors for buckling. The SSBR is assumed to be centrally attached to the boom.

2.5. Packaging Analyses

Finally the folding simulation of the SSBR is carried out to determine the stress and strain levels in folded configuration and to ensure that these values do not exceed the ultimate values of the material. During folding it is assumed that two diametrically opposite edges of the reflector are pulled towards each other by half their original distance. The reflector is then held folded by two tie cables. The simulation is a non-linear static analysis, carried out by imposing prescribed displacements to two pairs of nodes on the rim of the dish.

3. DEMONSTRATOR ANALYSES & EXPERIMENTS

Following many investigations into the SSBR concept, Tan et.al. [5] have recently designed and manufactured a 0.8 m diameter demonstrator with a curved stiffener, Fig. 1. Due to the size of the demonstrator, the mould had to be manufactured in three separate parts along the height of the dish. The three separate parts which were constructed from modelling board were then glued together using an epoxy adhesive to form a male mould.

The demonstrator was manufactured using the resin film infusion (RFI) process in which the dry triaxial fabric was laid up in between sheets of the semi-solid resin film supplied on release paper. The lay-up is then heated and pressure applied to allow the resin to first melt and then flow into the fabric. The HexPly 913 resin used is tacky or slightly adhesive at room temperature (with a tack life of 30 days at 23°C), and hence the prepreg is kept refrigerated to about -10°C until required. Before curing, the prepreg sheets were cut to form 8 sectors and laid up on the mould to form the reflecting surface. The reinforcements were then laid up as extra layers on the nonreflecting side. The structure was then cured in an autoclave at 125°C and at a pressure of 7 bar for 60 minutes – with a heat rate between 2°C - 8°C.

Surface accuracy measurements were performed using photogrammetry, while packaging experiments were conducted using an Instron testing machine with ball and socket connections to allow for free rotation of the loading point. Folding simulations were performed in ABAQUS under displacement controls.

4. RESULTS

4.1. Full Scale SSBR

The results of the thermal distortion analysis are presented in Table 1. The results demonstrate that load case LC1 is the worst single load case, producing an rms error of 2.84μm. The maximum RMS error due to thermal distortions is 3.52μm and is generated by the thermal load combination of LC1+LC2+LC3 i.e. the gradients in the x and through thickness directions and an absolute temperature of -150°C. The distortions due to this combined load case is illustrated in Fig. 5. It is interesting to note that the 'hot' thermal load combination of LC1+LC2+LC4 has an error of 2.85μm, the majority of which is caused by LC1.

The modal analyses results for the cases of the reflector attached to a rigid interface and to the boom are listed in Table 2 while the fundamental modes of both cases are shown in Fig. 6, these modes manifest

Mode	Rigid support (Hz)	Attached to boom (Hz)
1	1.66	1.10
2	1.82	1.24
3	1.86	1.66
4	2.01	1.82
5	4.22	1.93
6	4.64	2.11
7	5.32	4.20
8	5.98	4.68
9	10.20	5.33
10	10.53	5.91

TAB. 2: Eigen Frequencies of SSBR.

Acceleration direction	Displacement (cm)	Location
x	1.44	tip of skirt
y	1.42	tip of skirt
z	4.95	tip of skirt

TAB. 3: Response to Unit Step Acceleration Inputs (in x,y,z directions) of the SSBR Centrally Attached to the Boom.

themselves as bending about the y-axis when reflector fixed at the center and a rotation about the y-axis when reflector attached to the boom. The reflector fixed at geometric centre has a fundamental natural frequency of 1.66 Hz and as expected the attachment to the boom lowers the frequency to 1.10 Hz.

Transient analysis simulations provide the maximum displacement magnitudes and focal point displacements. Time integration is carried out for 4 s. The maximum displacement magnitudes always occur at the tip of the skirt, and are given in Table 3. Focal point displacements due to each acceleration input were computed for the time frame where the maximum displacement magnitudes occur and are listed in Table 4. A maximum displacement magnitude of 4.95 cm occurs at tip of stiffener when the reflector is attached to the boom. Maximum defocusing due to the acceleration along z-direction is 42.8 mm and is due to the fact that the boom itself has its lowest stiffness in this direction.

The static buckling analyses showed that the lowest buckling load corresponds to an acceleration of 13.2 m/s^2 in the z-direction, yielding a localized buckling of the unsupported section of the stiffener adjacent to the hinge region, see Fig. 7.

Fig. 8 shows the SSBR in its deployed and folded configurations; here the folded configuration has been translated to the center of the deployed configuration, for comparison. Due to the offset configuration of the reflector, the root end has a larger curvature than the

Load case	Best fit RMS (mm)	α (rad)	β (rad)	k_0(mm)	F(mm)
LC1	0.00284	-5.07E-04	-9.09E-04	3.496	4800.1
LC2	0.00020	-1.96E-05	1.56E-04	-0.137	4800.0
LC3	0.00037	5.62E-06	1.40E-05	-0.109	4800.2
LC4	0.00037	-4.91E-06	-1.28E-05	0.097	4799.8
LC1+LC2+LC3	0.00352	-5.13E-04	-8.51E-04	3.531	4800.3
LC1+LC2+LC4	0.00285	-5.24E-04	-8.78E-04	3.736	4799.9

TAB. 1: RMS Errors for Thermal Loads.

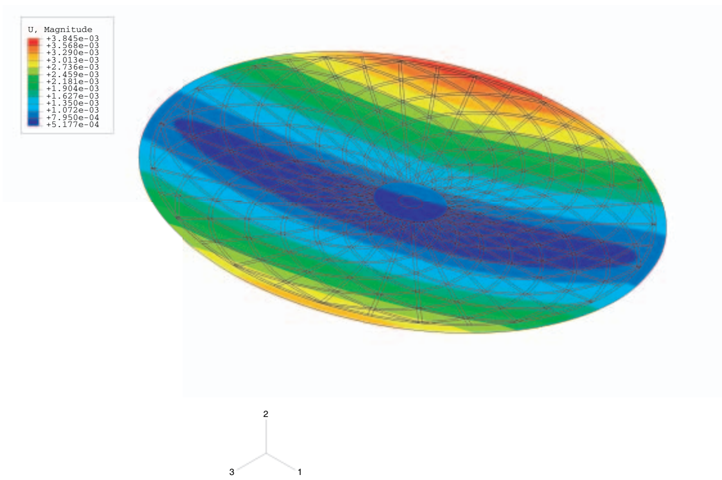

FIG. 5: Displacement Magnitudes due to Thermal Loading.

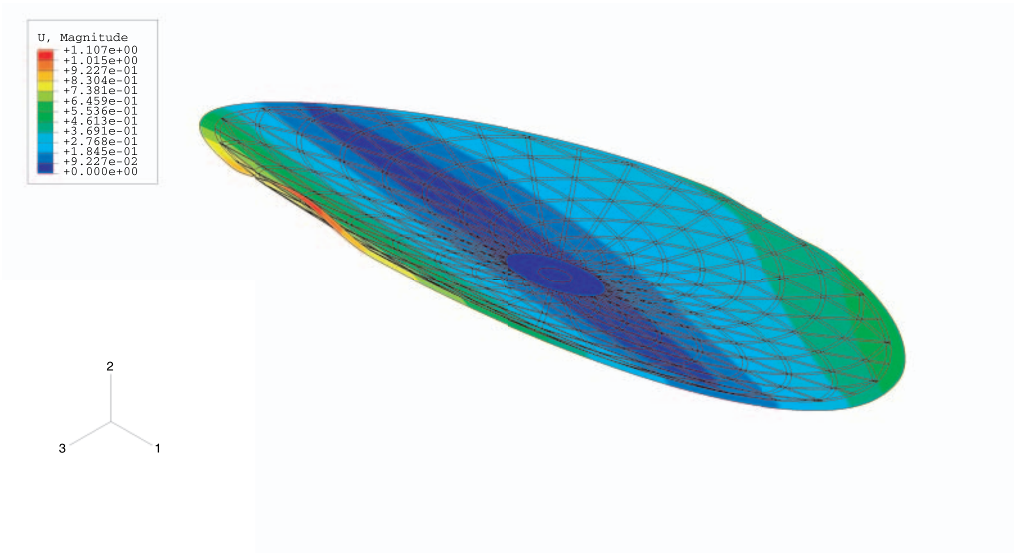

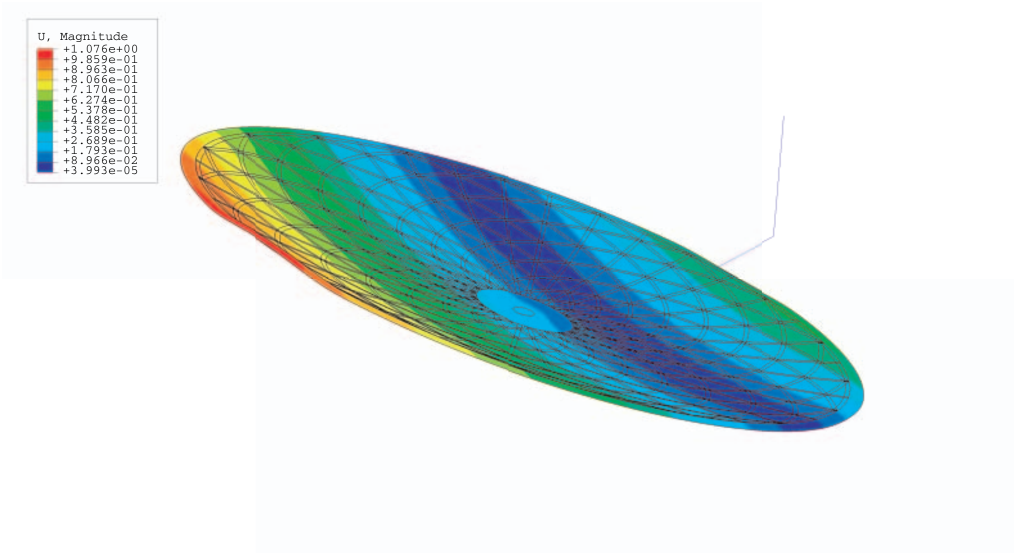

FIG. 6: Mode 1: (a) SSBR on a Rigid Interface, top, (b) SSBR attached to the boom, bottom

Acceleration direction	Defocusing (mm) x	y	z
x	12.5	-1.5	6.7
y	-0.1	10.8	-0.5
z	-42.8	-0.5	-19.5

TAB. 4: Defocusing due to Unit Step Accelerations.

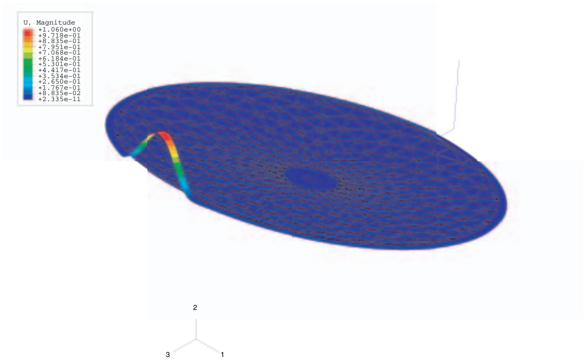

FIG. 7: First Buckling Mode of SSBR.

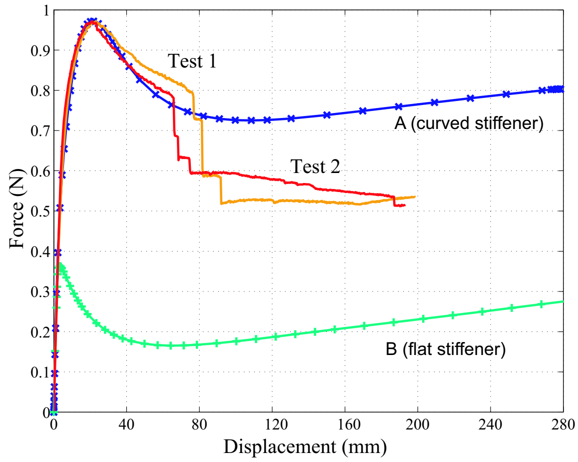

FIG. 9: Packaging Behaviour of Experimental and Finite Element Simulations for the 0.8m Demonstrator.

tip end in the deployed configuration, and this results in an unsymmetrical fold. In folded configuration, a maximum bending strain of 0.7% – safe from the viewpoint of material failure– occurs in the stiffener.

4.2. Small Scale Demonstrator

The resulting 0.8 m diameter stiffened reflector has a fundamental frequency of 12 Hz, and is extremely light weight, a mass of less than 100 grams.

The packaging experiments on the demonstrator showed good agreement between finite element and experimental results, especially for the initial stiffness regime and the peak snapping force, Fig. 9. The lines A and B are the force displacement responses of the finite element simulations, in which response A corresponds the demonstrator with the curved stiffener whereas response B corresponds an identical structure of an equal mass but with a flat horizontal rim stiffener, while the other lines are for the experimental results of the physical demonstrator. The peak packaging force is about 1 N while the rms surface accuracy was measured to be 0.78 mm and was mainly influenced by manufacturing errors in the mould. The 0.8 m demonstrator serves to verify both FE simulations and the feasibility of the concept.

5. CONCLUSIONS

The feasibility of the SSBR has been demonstrated through both comprehensive and extensive analyses showing that it is capable of meeting the stringent requirements for large reflector antennas and the construction and testing of a small scale demonstrator.

Packaging experiments of the demonstrator have been used to verify the FE model, good agreement between FE and experimental results was obtained for the initial stiffness regime but the instabilities involved in the buckling of the stiffener in the physical model proved difficult to model in the FE simulations and will be further investigated.

Besides having the lowest mass of 25.5 kg and highest deployed stiffness amongst the state of the art designs analysed in the ESA sponsored TAHARA study [1] the full scale SSBR also meets all the other specifications for high accuracy reflector antennas such as RMS error < 0.5 mm, reflector mass < 1.5 kg/m^2, package volume, deployment reliability. Furthermore it is expected to be able to operate at even higher frequencies than the Ku band design requirement. Tan [3] showed that the 4.6 m version has potential at operating at frequencies higher than Ka band.

ACKNOWLEDGEMENTS

The authors would like to acknowledge the financial support of the British Council under the Researcher Exchange Programme and also the generosity of Professor Sergio Pellegrino as some of the work presented here was performed while the authors were at the Deployable Structures Laboratory at the Cambridge University Engineering Department.

References

[1] Datashvili, L., Lang, M., Zauner, Ch., Baier, H., Soykasap, O., Tan, L.T., Kueh, A., and Pellegrino, S. Reflector Concepts Analysis. Technical

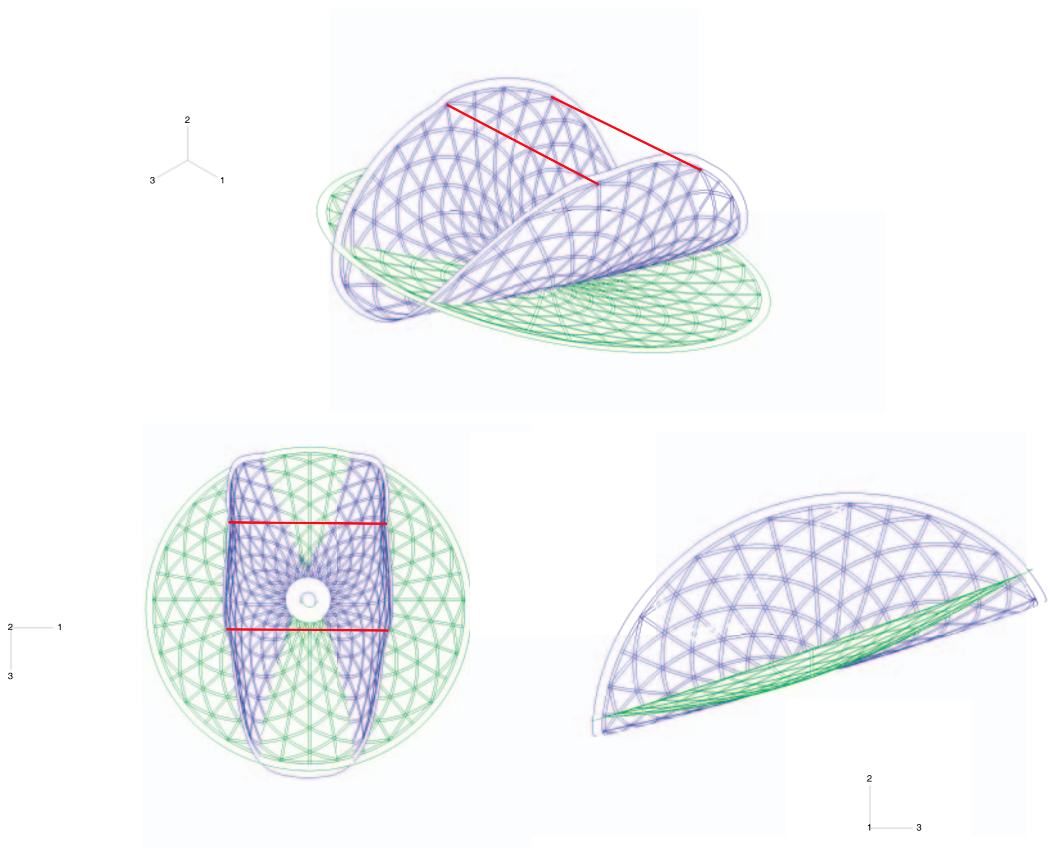

FIG. 8: SSBR in Deployed (Green) and Folded (Blue) Configurations; Tie Cables (Red).

Report WP1000, LLB-R-12/07/04-02D-02, Institute of Lightweight Structures, Aerospace Department, Technical University of Munich. For ESA Contract number 16757/02/NL/LvH/bj, "Technical Assessment of High Accuracy Large Space Borne Reflector Antenna" (TAHARA) (2004).

[2] Tan, L.T. and Pellegrino, S., Ultra thin deployable reflector antennas. In Proc. 45th AIAA/ASME/ASCE/AHS/ASC Structures, Structural Dynamics and Materials Conference, 19-22 April 2004, Palm Springs, CA AIAA 2004-1730.

[3] Tan, L.T., Thin-Walled Elastically Foldable Reflector Structures, Department of Engineering, University of Cambridge, 2002.

[4] Tan, L.T. and Pellegrino, S., Thin-Shell Deployable Reflectors with Collapsible Stiffeners Part 1: Approach, *AIAA Journal*, Vol. 44, No. 11, pp. 2515 – 2523, 2006.

[5] Tan, L.T., Soykasap, O., Pellegrino S. Design & Manufacture of Stiffened Spring-Back Reflector Demonstrator. In Proc. 46 th AIAA/ASME/ASCE/AHS/ASC Structures, Structural Dynamics and Materials Conference, Austin, TX , April 18 21, 2005, AIAA Paper 2005-2048.

[6] Hibbit, Karlsson and Sorensen, Inc., ABAQUS/Standard User's Manual, Version 6.4, Pawtucket, RI, USA, 2004.